0031-3998/09/6603-0301
PEDIATRIC RESEARCH

Vol. 66, No. 3, 2009
Printed in U.S.A.

Spontaneous Brain Activity in the Newborn Brain During Natural Sleep—An fMRI Study in Infants Born at Full Term

PETER FRANSSON, BEATRICE SKIÖLD, MATHIAS ENGSTRÖM, BOUBOU HALLBERG, MIKAEL MOSSKIN, ULRIKA ÅDEN, HUGO LAGERCRANTZ, AND MATS BLENNOW

Department of Clinical Neuroscience [P.F., M.E.], Stockholm Brain Institute, Karolinska Institute; Department of Woman and Child Health [B.S., B.H., U.Å., H.L.], Astrid Lindgren Children's Hospital, Karolinska Institute; Department of Neuroradiology [M.M.], Karolinska University Hospital, Stockholm, SE-171 76, Sweden; Department of Clinical Science [M.B.], Intervention and Technology, Karolinska Institute, Huddinge S-141 86, Sweden

ABSTRACT: Recent progress in functional neuroimaging research has provided the opportunity to probe at the brain's intrinsic functional architecture. Synchronized spontaneous neuronal activity is present in the form of resting-state networks in the brain even in the absence of external stimuli. The objective of this study was to investigate the presence of resting-state networks in the unsedated infant brain born at full term. Using functional MRI, we investigated spontaneous low-frequency signal fluctuations in 19 healthy full-term infants. Resting-state functional MRI data acquired during natural sleep was analyzed using independent component analysis. We found five resting-state networks in the unsedated infant brain born at full term, encompassing sensory cortices, parietal and temporal areas, and the prefrontal cortex. In addition, we found evidence for a resting-state network that enclosed the bilateral basal ganglia. **(*Pediatr Res* 66: 301–305, 2009)**

It is well known that the brain's energy expenditure is considerably larger than what is to be expected from its weight alone. Similar observations have been made in the infant brain (1). Moreover, it has also become apparent that the additional brain energy required to respond to changes in the environment is surprisingly small (2). Taken together, these observations have lead researchers to conclude that a large amount of the brain's activity is spent on tasks that as of yet is unaccounted for (3). Several theories related to the functional role of the brain's intrinsic activity have been proposed. Speculatively, intrinsic brain activity might be related to the neuronal activity necessary to retain a sustained level of maintenance and updating of information flow in the brain. To this end, recent development in functional MRI (fMRI) research has provided the opportunity to gain insights into the brain's intrinsic functional architecture by recording spontaneous, low-frequency blood oxygenation level dependent (BOLD) fMRI signal changes that are present during rest, *i.e.* in absence of any overt behavior (see Ref. 4 for a recent review). Several studies have shown that spontaneous changes in resting-state fMRI activity is related to the changes in neuronal activity (5,6) and that signal synchronicity across widely separated brain areas exist within multiple so-called resting-state networks in the adult brain (7). Previous reports have shown that functional connectivity in the format of resting-state networks in the adult brain spans brain regions that are involved in sensory perception (8–10), language (11), and in the so-called default-mode network (12–14). The default-mode network is believed to be involved in different aspects of self-referential mental efforts (see Ref. 15; for a recent review on the mental capabilities of the newborn infant see Ref. 16). Recently, a number of studies have addressed the possibility to use resting-state functional connectivity as a biomarker for neurologic deficits in spatial neglect after stroke in the parietal cortex (17) as well as its potential role in developmental disorders such as attention deficit hyperactivity disorder and autism (see Ref. 18 for a recent review).

Because the resting-state fMRI does not require any overt feedback by the subjects, it is well suited to study functional connectivity in clinical populations as well as in children and infants. In a recently published study, we could show that spontaneous low-frequency fMRI BOLD signals are present in the sedated infant brain (19). In detail, using a model-free explorative image analysis method, we could show for the first time that the infant brain through spatio-temporal synchronization of spontaneous signal fluctuations exhibited resting-state networks that spanned long-range cortical areas that among others are known to be involved in sensory perception. However, our previous study was conducted at term-corrected age in infants born preterm (gestational age $<$27 wk) and lightly sedated (choral hydrate, 30 mg/kg). Hence, it is conceivable that preterm birth or prenatal factors might have influenced our results. Similarly, the effect of sedation on resting-state activity is currently under investigation and a modulation of functional connectivity from sedative agents cannot be ruled out (20–23). Therefore, the aim in this work was to investigate resting-state networks in the infant brain during natural sleep in babies born at term.

Received February 11, 2009; accepted May 19, 2009.

Correspondence: Peter Fransson, Ph.D., MR Research Center, N8, Department of Clinical Neuroscience, Karolinska University Hospital, Stockholm SE-171 76, Sweden; e-mail: Peter.Fransson@ki.se

Supported by a grant from the Karolinska Institute research foundation (P.F.) and from the Swedish Medical Research Council (2006-60612101), Jerring Foundation, Linnea and Josef Carlsson's Foundation, Frimurarorden Foundation, and Karolinska University Hospital (SLL 20060464) (U.Å, H.L., B.H., B.S. and M.B).

Abbreviations: BOLD, blood oxygenation level dependent; **CS,** caesarean section; **EPI,** echo planar imaging; **fMRI,** functional MRI; **PICA,** probabilistic independent component analysis

PATIENTS AND METHODS

Participants. All 21 infants included in this study were born at term. Only healthy mothers with uncomplicated pregnancies, giving birth to healthy babies with normal Apgar scores, were invited to enter the study. Subjects were recruited from two hospitals in the Stockholm area. Parents with planned caesarean section (CS) were informed about the study. If parents were interested in participating in this study, a doctor further informed the family on the details regarding the MR examination. The reasons for CS were uncomplicated breech presentation, prior CS (acute or planned), history of abdominal surgery or anxiety/fear of delivery (humanitarian CS). No infants were delivered with acute CS. All infants except one were delivered with CS and informed consent was received from all parents. All MR scanning was conducted when the infants were in a stage of natural sleep. To facilitate sleep and successful scanning, all subjects were fed just before the MRI examination. Anatomical MR images were analyzed by an experienced pediatric neuroradiologist and all MR scans were found to be normal without any visible brain abnormalities. The study was approved by the regional ethical committee in Stockholm. The infants comfort during scanning was secured by a pediatrician who resided inside the scanning room during the complete imaging session. Arterial oxygen saturation and heart rate were continuously measured during scanning. All included infants were appropriate for their gestational age with regard to birth weight, height, and head circumference. Further details regarding the infants are given in Table 1.

MR image acquisition. A Philips Intera 1.5 Tesla scanner equipped with a 6-channel receive-only coil was used to acquire both anatomical and fMRI in all studied infants. MR image acquisition parameters were closely matched to the settings used in our previous study in preterm infants (19). Briefly, fMRI of the infant brain were acquired by means of an echo planar image (EPI) sequence sensitized to T2*-weighted BOLD signal changes (TR/TE/flip, 2000 ms/50 ms/80 degrees; matrix size, 64 × 64; field-of-view, 180 × 180 mm). Each EPI volume comprised 20-axial slices (slice thickness = 4.5 mm, interleaved slice acquisition order) yielding a spatial resolution of 2.8 × 2.8 × 4.5 mm^3. Resting-state functional connectivity was assessed by recording BOLD signal changes during 10 min of sleep (300 EPI volumes). Four dummy scans were included in the beginning of each fMRI scanning session to achieve steady-state magnetization. Anatomical MRI included a T1-weighted turbo-spin echo scan, an inversion recovery scan as well as a high-resolution three-dimensional gradient-echo image sequence (TR/TE/flip, 40 ms/4.6 ms/30 degrees; acquired voxel size, 0.9 × 0.9 × 1 mm^3; reconstructed to 0.7 × 0.7 × 1 mm^3). Additionally, T2-weighted turbo-spin-echo images were acquired in sagittal, coronal, and axial slice orientations. The total scanning time amounted to approximately 50 min. Noise protection was provided using a 4-fold protection system including standard pediatric muffs, a dental putty molded into the hearing canal (Affinis dental putty soft, Coltene AG, Switzerland), minimuffs (Natus Medical Inc, San Carlos, CA), and a custom-made acoustic hood (thickness = 104 mm) made from polyurethane that attached tightly to the upper semicircle of the magnet bore.

Table 1. *Parameters for the infants included in the study*

Subject number	Gender	BW (g)	GA (w + d)	GA at MRI	Delivery	H-CIRC at MRI (cm)	Hospital
1	M	3714	38w5d	39w6d	CS	36	KH
2	M	3790	38w6d	39w6d	CS	38.5	KH
3	F	3300	38w5d	40w2d	CS	36.0	DH
4	F	4055	38w6d	40w4d	CS	37	DH
5	F	3075	38w5d	40w2d	CS	35.5	DH
6*	M	3480	39w1d	40w4d	CS	37.0	DH
7	F	3560	38w5d	40w2d	CS	36.5	DH
8	F	4100	38w5d	40w3d	CS	36.0	DH
9	M	4020	39w0d	40w3d	CS	36.0	DH
10	F	3680	38w4d	40w1d	CS	35.0	DH
11	F	2664	38w6d	40w3d	CS	34.0	KH
12	M	3850	38w6d	41w1d	CS	36.5	DH
13	M	4025	38w5d	41w2d	CS	36.0	DH
14*	F	3680	38w5d	40w1d	CS	35.5	DH
15	M	3630	38w6d	40w3d	CS	35.0	DH
16	F	4045	39w1d	41w6d	CS	36.5	DH
17	M	3435	37w4d	39w2d	CS	34.5	DH
18	F	2855	38w6d	41w5d	CS	35.5	DH
19	F	3405	39w6d	40w5d	VD	35.0	DH
20	F	3385	38w3d	40w6d	CS	35	DH
21	M	3670	38w3d	40w6d	CS	37.5	DH

VD, vaginal delivery; H-CIRC, head circumference; GA, gestational age; BW, birth weight; DH, Danderyd Hospital; KH, Karolinska Hospital; M, male; F, female.

* Data not used.

Image preprocessing. Postacquisition image processing closely followed the steps outlined in our previous study (19). In brief, nonbrain voxels were excluded (24) followed by correction for subject movement, spatial normalization to an infant T2-weighted template (25), and spatial smoothing (full width at half maximum = 6 mm) within the SPM2 software package (Wellcome Trust Center for Neuroimaging, University College London, UK, Ref. 26). In 10 of 21 subjects, subject movement during scanning was small throughout the whole scanning session with a maximal translational movement of less than 1 mm and a maximal rotational movement of less than 1.5 degrees across all 10 infants. In nine subjects, the realignment procedure showed one or two episodes of brief, sudden jerk-like movements during which the infants head was tilted away from the original position and within 10–30 s titled back again in a position that was very close in space to the original position. For these nine subjects, the image data were treated in same manner as in our previous study (19). Accordingly, the affected image volumes were removed from the fMRI dataset and the remaining image volumes were treated as one continuous dataset (27). The remaining two subjects showed excessive movement throughout the scanning session and the corresponding datasets were discarded. Thus, our final data analysis was performed on 200 fMRI EPI volumes obtained in 19 subjects.

Image analysis. Intrinsic brain activity at rest in the infant brain was estimated using the temporal concatenation version of the tensorial probabilistic approach to independent component analysis (PICA) as implemented in the MELODIC (version 4.0) module in the FSL software package (Oxford Centre for functional MRI of the Brain, FMRIB, UK, Ref. 28). Independent component analysis is a multivariate method that does not require any seed regions specified by the user to measure functional connectivity (29). Specifically, PICA divides the four-dimensional EPI data into spatially non-Gaussian processes in the presence of Gaussian noise and uses a Gaussian mixture model to test for significance of the extracted spatial maps (30). The alternative hypothesis was tested at $p > 0.5$ for "activation" *versus* null to create thresholded results for each spatial map. Besides the ability to produce spatio-temporal components that are likely to be candidates for resting-state networks, ICA is able to divide resting-state fMRI data into maps that show strong resemblance, in both the spatial and temporal domain, to maps typically assigned to other signal sources such as subject motion and non-neuronal physiologic noise. The independent components here shown to represent resting-state networks were selected on the basis of anatomical localization and frequency content. In detail, information from the anatomical localization was used as far as those components that exhibited activity pattern that mainly resided in known major blood vessels, *e.g.* in the vicinity of the circle of Willis, were discarded. Similarly, components that showed "rim"-like activation patterns typical of subject motion were not considered further. Components for which approximately more than 50% of the activity was judged to reside in gray matter were considered to be of interest. Furthermore, only components for which the majority of the signal variance resided below 0.1 Hz were considered to be relevant.

RESULTS

On the basis of the results from the 19 subjects included in the independent component analysis, we could identify six anatomically coherent resting-state networks with the majority of the signal variance residing in the frequency interval of 0.01–0.05 Hz. An example of the resting-state networks typically observed in individual subjects is shown in Figure 1, whereas the group results are shown in Figure 2. Coherent synchronization of low-frequency intrinsic brain activity was found in the middle part of the occipital cortex (Figs. 1*A* and 2*A*), bilateral sensorimotor cortex (Figs. 1*B* and 2*B*), bilateral temporal cortex (Figs. 1*C* and 2*C*), middle and lateral aspects of the parietal cortex (Figs. 1*D* and 2*D*), anterior prefrontal cortex (Figs. 1*E* and 2*E*), and bilateral basal ganglia (Figs. 1*F* and 2*F*). The relative amount of variance explained by each network in relation to the total amount of variance was 1.63% (visual cortex, Fig. 2*A*), 3.18% (sensorimotor cortex, Fig. 2*B*),

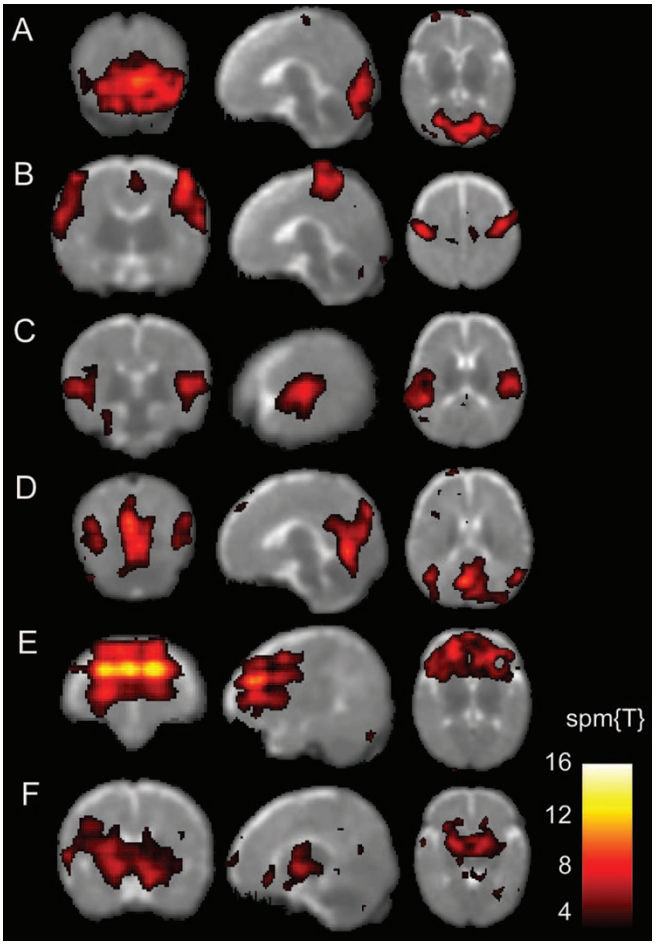

Figure 1. Intrinsic brain networks found in a typical infant born at term based on a probabilistic independent component analysis of fMRI acquired during sleep. Each row shows in a coronal, sagittal and axial view resting-state networks thresholded at $p > 0.5$ (alternative-hypothesis threshold for activation *vs* null) superimposed on a T2-weighted MR image infant brain template. At the individual level, resting-state networks were found in primary visual areas (*A*), bilateral sensorimotor regions (*B*), bilateral temporal/inferior parietal cortex including the primary auditory cortex (*C*), posterior lateral and midline aspects of the parietal cortex (*D*), medial and lateral parts of the prefrontal cortex (*E*), and in bilateral subcortical regions (*F*). The left side of the image corresponds to the left side of the brain. The color-bar shows the corresponding t-value.

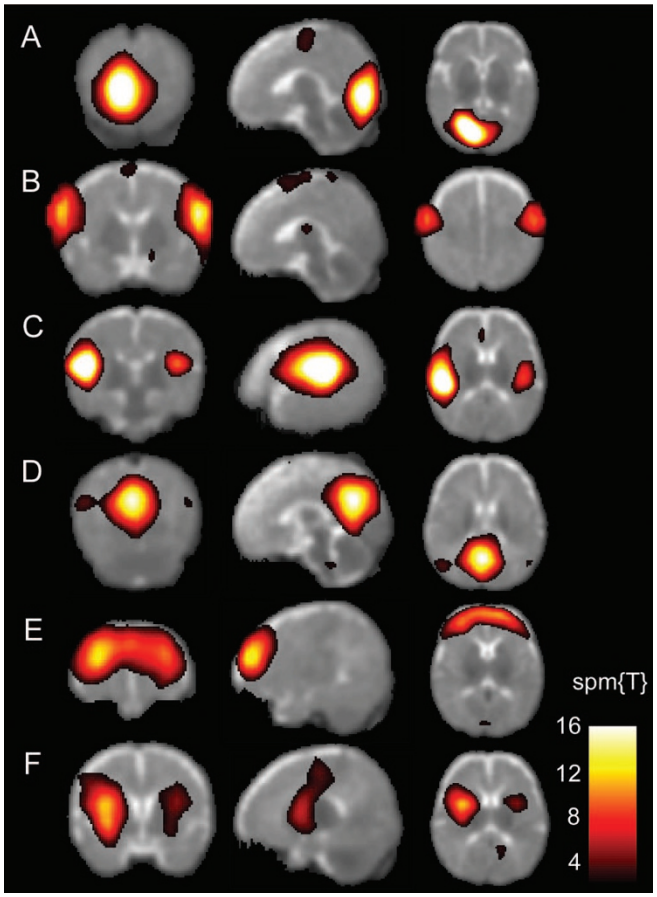

Figure 2. Group consistent intrinsic brain networks in the infant born at term based on an independent component analysis of fMRI acquired during sleep. Each row shows in a coronal, sagittal and axial view resting-state networks thresholded at $p > 0.5$ (alternative-hypothesis threshold for activation *vs* null) superimposed on a T2-weighted MR image infant brain template. Resting-state networks at a group level were found in primary visual areas (*A*), bilateral sensorimotor regions (*B*), bilateral temporal/inferior parietal cortex including the primary auditory cortex (*C*), posterior lateral and midline aspects of the parietal cortex (*D*), medial and lateral parts of the prefrontal cortex (*E*), and in the bilateral basal ganglia (*F*). The left side of the image corresponds to the left side of the brain. The color-bar shows the corresponding t-value.

0.70% (temporal cortex, Fig. 2*C*), 4.78% (parietal cortex, Fig. 2*D*), 1.60% (anterior prefrontal cortex, Fig. 2*E*), and 0.1% (basal ganglia, Fig. 2*F*).

DISCUSSION

Overall, our current results are in good agreement with our previous investigation of resting-state activity in sedated preterm infants (19). The spatial distributions of the resting-state networks that encompasses primary sensory cortices (Figs. 1*A–C* and 2*A–C*) are very similar to the networks obtained in preterm infants (see for reference Fig. 3A–C in Ref. 19). Further, this observation is in agreement with previous investigations that have shown resting-state networks present in visual, auditory, and sensorimotor areas in the adult brain (7–9,31). Moreover, the network consisting of the medial as well as the lateral parts of the parietal cortex depicted in Figures 1*D* and 2*D* was also found in sedated preterm infants, although no involvement of the cerebellum was found in naturally sleeping infants born at full term. Similarly, the anterior network shown in Figures 1*E* and 2*E* was also found in sedated preterm infants as well as in adults (7,32,33). Interestingly, the resting-state network shown in Figures 1*F* and 2*F* that resides predominately in the basal ganglia was not detected in sedated infants born preterm. This is a novel finding in infants born at term and it is in accordance with a recent study that found a strong bilateral resting-state pattern in the caudatus and putamen in adults (34). At this stage, we consider it too early to relate the absence of resting-state activity in the basal ganglia in our previous study to any factor related to preterm birth or sedation. This is due to the fact that primarily the study performed in preterm babies used a rather small sample size, yielding a too limited sensitivity to adequately address this discrepancy. Further studies using larger cohorts of subjects need to be carried out to address this issue.

Thus, the overall impression from our current findings is that they corroborate our previous results in that low-frequency fMRI signal fluctuations are present and mediate long-range functional connectivity already in the infant brain.

The presence of bilateral functional connectivity patterns in primary sensory brain areas are also supported by a recent study by Lin *et al.* (35) that reported bilateral resting-state connectivity in sensory areas in 38 neonates. However, our recurrent finding of a bilateral resting-state activity pattern in the sensorimotor region in the infant brain as well as the results presented by Lin *et al.* are to some extent in contrast to the results reported recently by Liu *et al*. (36). In the Liu study, fMRI was performed in sleeping 1-y-old children and they reported a bilateral activity pattern similar to the pattern shown here in Figures 1*B* and 2*B* in only two of 11 subjects, whereas the remaining subjects showed a predominately intrahemispheric resting-state pattern in the sensorimotor region. The authors suggested that the fact that we investigated infants born preterm as well as different levels of sleep were induced, *i.e.* sedation *versus* nonsedation, might have contributed to the observed differences. However, both factors were addressed in this study and our present findings of strongly interhemispheric resting-state patterns corroborate our previous results obtained in sedated infants born preterm. It therefore seems unlikely that the unilateral resting-state pattern reported by Liu *versus* the bi-laterality found in our studies as well as in the Lin study is due to any of the suggested factors. It should also be noted that although the sensorimotor resting-state network obtained in the majority of the infants investigated by Liu *et al.* showed a predominately lateralized pattern, a small but still significant cluster was also found in the contralateral hemisphere (see Fig. 2*A* and *B* in Ref. 36. for comparison). It is likely that the relatively small sample sizes used together with small differences in image analysis strategies might have contributed to the observed differences.

One of the resting-state networks commonly observed in the adult brain that have received much attention is the so-called default-mode network (12–14,37). The default-mode network comprises the medial aspects of the prefrontal cortex, precuneus/posterior cingulate cortex, bilateral parietal cortex, and the lateral and medial temporal cortex. There is a growing interest to understand its role in the brain's functional architecture and how the default network may be affected in disease (see refs. 15 and 18 for recent reviews). Similar to our previous investigation in infants born preterm, we observed what tentatively might be called a proto-default network in the infant brain with a rather strong resting-state functional connectivity between the precuneus/posterior cingulate cortex and the bilateral parietal cortex. However, at a group level, no significant functional connectivity between the posterior/medial aspects of the parietal cortex and the medial prefrontal cortex was observed and no significant connectivity with the temporal cortex was found (Figs. 1*D* and 2*D*). This finding is consistent with the idea that the default network matures gradually throughout infancy, childhood, and adolescence (38). The relative strong functional connectivity between the medial and the lateral parietal cortex in the proto-default network (Figs. 1*D* and 2*D*) is interesting in the view of recent research on cortical hubs in the adult brain. It has been hypothesized that cortical hubs, *i.e.* brain regions that show a high degree of centrality in cortical networks including a large degree of anatomical and functional connectivity, play a pivotal role in coordination, and integration of information flow in the brain (39). With regard to the default network, recent MRI work in the adult brain have shown that the precuneus/posterior cingulate cortex exhibit a high degree of both anatomical (40,41) and functional connectivity (42), thus making it a likely candidate for being a cortical hub in the default network. On the basis of the present findings in infants, we tentatively suggest that the maturation of functionally central cortical hubs starts already in infancy.

It is also worth noting that the observed resting-state functional connectivity in infants born at term was recorded during natural sleep. To this end, it is well known that natural sleep consists of several stages, each characterized with its own electroencephalographic signature. Previous work using EEG as well as fMRI has shown that the depth of sleep have an effect on resting-state functional connectivity (43). A recent study have shown that a transition from wakefulness to light sleep introduce a slight increase in functional connectivity in networks that include higher order cortices (44). Similarly, during light sleep compared with wakefulness, increases in functional connectivity in networks residing in primary sensory cortices have been reported (22). Hence, it is conceivable that differences in arousal are related to the observed differences in resting-state connectivity between adults and infants. Moreover, the depth of sleep was not controlled for in this study, and it cannot be ruled out that some of the differences in functional connectivity between naturally sleeping infants born at full-term and sedated infants born preterm can be attributed to depth of sleep.

In conclusion, we could show that the infant brain born at term hosts resting-state networks driven by spontaneous changes in neuronal activity. Our results showed that neither preterm birth nor light sedation seems to have a detrimental influence on the resting-state patterns in the infant brain. We could corroborate our previous findings from the infants born preterm in that several cortical as well as subcortical long-range functional networks mediated via synchronous spontaneous low-frequency BOLD fMRI signal fluctuations are present in the infant brain born at term. Because it has recently been shown that resting-state functional connectivity reflects structural connectivity in the adult brain (45,46), we suggest that mapping of resting-state networks can potentially be used as a tool to probe white matter integrity in the brain. In future studies, we aim to investigate the relationship between anatomical connectivity and resting-state functional connectivity in the infant brain as well as examining the influence from white matter abnormalities typically observed in preterm infants on resting-state functional connectivity.

Acknowledgments. We thank Rose Mari Claesson and Elinor Ihre for their assistance in MRI scanning.

REFERENCES

1. Settergren G, Lindblad BS, Persson B 1980 Cerebral blood flow and exchange of oxygen, glucose ketone bodies, lactate, pyruvate and amino acids in anesthetized children. Acta Paediatr Scand 69:457–465
2. Raichle ME, Mintun MA 2006 Brain work and brain imaging. Annu Rev Neurosci 29:449–476
3. Raichle ME 2006 The brain's dark energy. Science 314:1249–1250
4. Fox MD, Raichle ME 2007 Spontaneous fluctuations in brain activity observed by functional magnetic resonance imaging. Nat Rev Neurosci 8:700–711
5. Shmuel A, Leopold DA 2008 Neuronal correlates of spontaneous fluctuations in fMRI signals in monkey visual cortex: implications for functional connectivity at rest. Hum Brain Mapp 29:751–761
6. Johnston JM, Vaishnavi SN, Smyth MD, Zhang D, He BJ, Zempel JM, Shimony JS, Snyder AZ, Raichle ME 2008 Loss of resting interhemispheric functional connectivity after complete section of the corpus callosum. J Neurosci 28:6453–6458
7. Damoiseaux JS, Rombouts SA, Barkhof F, Scheltens P, Stam CJ, Smith SM, Beckmann CF 2006 Consistent resting-state networks across healthy subjects. Proc Natl Acad Sci USA 103:13848–13853
8. Biswal B, Yetkin FZ, Haughton VM, Hyde JS 1995 Functional connectivity in the motor cortex of resting human brain using echo-planar MRI. Magn Reson Med 34:537–541
9. Lowe MJ, Mock BJ, Sorensen JA 1998 Functional connectivity in single and multislice echoplanar imaging using resting-state fluctuations. Neuroimage 7:119–132
10. Cordes D, Haughton VM, Arfanakis K, Wendt GJ, Turski PA, Moritz CH, Quigley MA, Meyerand ME 2000 Mapping functionally related regions of brain with functional connectivity MR imaging. AJNR Am J Neuroradiol 21:1636–1644
11. Hampson M, Peterson BS, Skudlarski P, Gatenby JC, Gore JC 2002 Detection of functional connectivity using temporal correlations in MR images. Hum Brain Mapp 15:247–262
12. Greicius MD, Krasnow B, Reiss AL, Menon V 2003 Functional connectivity in the resting brain: a network analysis of the default mode of brain function. Proc Natl Acad Sci USA 100:253–258
13. Fransson P 2005 Spontaneous low-frequency BOLD signal fluctuations: an fMRI investigation of the resting-state default mode of brain function hypothesis. Hum Brain Mapp 26:15–29
14. Fox MD, Snyder AZ, Vincent JL, Corbetta M, Van Essen DC, Raichle ME 2005 The human brain is intrinsically organized into dynamic, anticorrelated functional networks. Proc Natl Acad Sci USA 102:9673–9678
15. Buckner RL, Andrews-Hanna JR, Schacter DL 2008 The brain's default network: anatomy, function and relevance to disease. Ann N Y Acad Sci 1124:1–38
16. Lagercrantz H, Changeux JP 2009 The emergence of human consciousness: from fetal and neonatal life. Pediatr Res 65:255–260
17. He BJ, Snyder AZ, Vincent JL, Epstein A, Shulman GL, Corbetta M 2007 Breakdown of functional connectivity in frontoparietal networks underlies behavioural deficits in spatial neglect. Neuron 53:905–918
18. Greicius MD 2008 Resting-state functional connectivity in neuropsychatric disorders. Curr Opin Neurol 21:424–430
19. Fransson P, Skiöld B, Horsch S, Nordell A, Blennow M, Lagercrantz H, Åden U 2007 Resting-state networks in the infant brain. Proc Natl Acad Sci USA 104:15531–15536
20. Fukunaga M, Horovitz SG, van Gelderen P, de Zwart JA, Jansma JM, Ikonomidou VN, Chu R, Deckers RH, Leopold DA, Duyn JH 2006 Large-amplitude, spatially correlated fluctuations in BOLD fMRI signals during extended rest and early sleep stages. Magn Reson Imaging 24:979–992
21. Vincent JL, Patel GH, Fox MD, Snyder AZ, Baker JT, Van Essen DC, Zempel JM, Snyder LH, Corbetta M, Raichle ME 2007 Intrinsic functional architecture in the anaesthetized monkey brain. Nature 447:83–86
22. Horovitz SG, Fukunaga M, de Zwart JA, van Gelderen P, Fulton SC, Balkin TJ, Duyn JH 2008 Low frequency BOLD fluctuations during resting wakefulness and light sleep: a simultaneous EEG-fMRI study. Hum Brain Mapp 29:671–682
23. Greicius MD, Kiviniemi V, Tervonen O, Vainionpää, Alahutha S, Reiss AL, Menon V 2008 Persistent default-mode network connectivity during light sedation. Hum Brain Mapp 29:839–847
24. Smith SM 2002 Fast robust automated brain extraction. Hum Brain Mapp 17:143–155
25. Dehaene-Lambertz G, Dehaene S, Hertz-Pannier L 2002 Functional neuroimaging of speech in infants. Science 298:2013–2015
26. Friston KJ, Holmes AP, Worsley KP, Poline JB, Frith CD, Frackowiak RS 1994 Statistical parametrical maps in functional neuroimaging: a general linear approach. Hum Brain Mapp 2:189–210
27. Fair DA, Schlaggar BL, Cohen AL, Miezin FM, Dosenbach NU, Wenger KK, Fox MD, Snyder AZ, Raichle ME, Petersen SE 2007 A method for using blocked and event-related fMRI data to study "resting-state" functional connectivity. Neuroimage 35:396–405
28. Beckmann CF, Smith SM 2005 Tensorial extensions of independent component analysis of multi-subject fMRI analysis. Neuroimage 25:294–311
29. Calhoun VD, Kiehl KA, Pearlson GD 2008 Modulation of temporally coherent brain networks estimated using ICA at rest and cognitive tasks. Hum Brain Mapp 29:828–838
30. Beckmann CF, Smith SM 2004 Probabilistic independent component analysis for functional magnetic resonance imaging. IEEE Trans Med Imaging 23:137–152
31. Tian L, Jiang T, Liu Y, Yu C, Wang K, Zhou Y, Song M, Li K 2007 The relationship within and between the extrinsic and intrinsic systems indicated by resting state correlational patterns of sensory cortices. Neuroimage 36:684–690
32. Beckmann CF, DeLuca M, Devlin JT, Smith SM 2005 Investigations into resting-state connectivity using independent component analysis. Philos Trans R Soc Lond B Biol Sci 360:1001–1013
33. van den Heuvel M, Mandl R, Hulshoff Pol H 2008 Normalized cut group clustering of resting-state fMRI data. PLoS One 3:e2001
34. Di Martino A, Scheres A, Margulies DS, Kelly AM, Uddin LQ, Shehzad Z, Biswal B, Walters JR, Castellanos FX, Milham MP 2008 Functional connectivity of human striatum: a resting-state fMRI study. Cereb Cortex 18:2735–2747
35. Lin W, Zhu Q, Gao W, Chen Y, Toh Ch, Styner M, Gerig G, Smith JK, Biswal B, Gilmore JH 2008 Functional connectivity MR imaging reveals cortical functional connectivity in the developing brain. AJNR Am J Neuroradiol 29:1883–1889
36. Liu WC, Flax JF, Guise KG, Sukul V, Benasich AA 2008 Functional connectivity of the sensorimotor area in naturally sleeping infants. Brain Res 1223:42–49
37. Raichle ME, MacLeod AM, Snyder AZ, Powers WJ, Gusnard DA 2001 A default mode of brain function. Proc Natl Acad Sci USA 98:676–682
38. Fair DA, Cohen AL, Dosenbach NU, Church JA, Miezin FM, Barch DA, Raichle ME, Petersen SE, Schlaggar BL 2008 The maturing architecture of the brain's default network. Proc Natl Acad Sci USA 105:4028–4032
39. Sporns O, Honey CJ, Kötter R 2007 Identification and classification of hubs in brain networks. PLoS One 2:e1049
40. Hagmann P, Cammoun L, Gigandet X, Meuli R, Honey CJ, Van Wedeen J, Sporns O 2008 Mapping the structural core of the human cerebral cortex. PLoS Biol 6:e159
41. Gong G, He Y, Concha L, Lebel C, Gross DW, Evans AC, Beaulieu C 2009 Mapping anatomical connectivity patterns of human cerebral cortex using in vivo diffusion tensor imaging tractography. Cereb Cortex 19:524–536
42. Fransson P, Marrelec G 2008 The precuneus/posterior cortex cingulate cortex plays a pivotal role in the default mode network: evidence from a partial correlation network analysis. Neuroimage 42:1178–1184
43. Dang-Vu TT, Schabus M, Desseilles M, Albouy G, Boly M, Darsaud A, Gais S, Rauchs G, Sterpenich V, Vandewalle G, Carrier J, Moonen G, Balteau E, Degueldre C, Luxen A, Philips C, Maquet P 2008 Spontaneous neural activity during human slow wave sleep. Proc Natl Acad Sci USA 105:15160–15165
44. Larson-Prior LJ, Zempel JM, Nolan TS, Prior FW, Snyder AZ, Raichle ME 2009 Cortical network functional connectivity in the decent to sleep. Proc Natl Acad Sci USA 106:4489–4494
45. Greicius MD, Supekar K, Menon V, Dougherty RF 2009 Resting-state functional connectivity reflects structural connectivity in the default mode network. Cereb Cortex 19:72–78
46. Skudlarski P, Jagannathan K, Calhoun VD, Hampson M, Skudlarska BA, Pearlson G 2008 Measuring brain connectivity: diffusion tensor imaging validates resting state temporal correlations. Neuroimage 43:554–561